

WATERFLOW: EXPLICIT PHYSICS-PRIOR RECTIFIED FLOW FOR UNDERWATER SALIENCY MASK GENERATION

Runting Li^{1*} Shijie Lian^{2*} Hua Li^{1†} Yutong Li¹ Wenhui Wu³ Sam Kwong⁴

¹Hainan University, China ²Huazhong University of Science and Technology, China
³Shenzhen University, China ⁴Lingnan University, Hong Kong

ABSTRACT

Underwater Salient Object Detection (USOD) faces significant challenges, including underwater image quality degradation and domain gaps. Existing methods tend to ignore the physical principles of underwater imaging or simply treat degradation phenomena in underwater images as interference factors that must be eliminated, failing to fully exploit the valuable information they contain. We propose WaterFlow, a rectified flow-based framework for underwater salient object detection that innovatively incorporates underwater physical imaging information as explicit priors directly into the network training process and introduces temporal dimension modeling, significantly enhancing the model’s capability for salient object identification. On the USOD10K dataset, WaterFlow achieves a **0.072** gain in S_m , demonstrating the effectiveness and superiority of our method. <https://github.com/Theo-polis/WaterFlow>.

Index Terms— Underwater Salient Object Detection, Rectified Flow, Physical prior, Generative model

1. INTRODUCTION

Underwater salient object detection aims to automatically identify and localize the most important or attention-grabbing objects in underwater images or videos [1]. Due to its significant applications in marine biology research, underwater robot navigation, environmental monitoring, and ocean exploration, it has been attracting increasing attention [2][3][4].

Currently, thanks to large-scale datasets and high-quality annotations, the field of salient object detection in terrestrial scenarios has made remarkable progress [5][6][7]. However, its counterpart in underwater environments faces considerable challenges, mainly due to the following reasons: 1) underwater images captured by devices often suffer from various types of degradation, such as color distortion, detail blurring, and contrast loss, which weaken the saliency of objects and hinder accurate foreground localization; 2) the marine environment differs greatly from terrestrial environments, exhibiting obvious domain shifts, and thus the direct transfer of terrestrial salient object detection techniques to underwater scenes often leads to unsatisfactory performance [2][8].

In recent years, generative models, particularly diffusion models [9], have demonstrated remarkable performance across a variety of computer vision tasks [10][11]. Diffusion models, by learning the generative process of data distributions, are capable of handling uncertainties within the data and producing high-quality and diverse samples, which hold significant potential for underwater salient object detection. However, applying diffusion models directly to un-

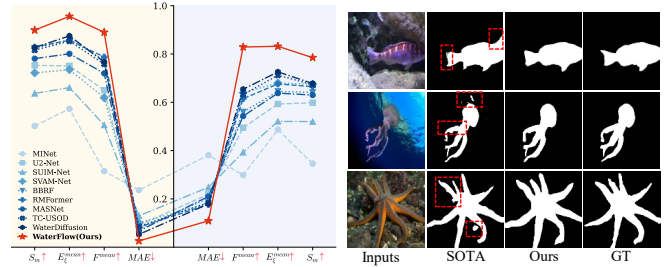


Fig. 1: The left panel shows the performance of our model on the **USOD10K(L)** and **UFO-120(R)** datasets, while the right panel compares our method against the previous SOTA approaches [10]. Red boxes highlight segmentation errors.

derwater object detection is hindered by computational inefficiency and unstable training. Traditional diffusion models typically require a large number of sampling steps to produce high-quality results, which is impractical for real-time underwater applications.

Moreover, many deep learning-based segmentation methods mainly focus on network architectures and feature modeling from a general computer vision perspective [12][13][14]. The imaging process follows complex physical principles, including dual attenuation from direct transmission and backscattering, wavelength-dependent scattering, and depth-induced color distortion [8]. These processes not only degrade image quality but also contain rich information about scene structure and object characteristics. Some studies have attempted to leverage these physical principles by treating image degradations as noise to be removed [15][3]. Although this can yield visually clearer images, it may also discard valuable information and introduce artificial artifacts. Other approaches adopt multi-task learning frameworks to jointly optimize enhancement and segmentation [10], but the discrepancy between the two objectives often leads to optimization challenges and increased model complexity. Inspired by these observations, we argue that the underwater imaging process itself encodes valuable priors which, if properly utilized, can enhance both learning efficiency and generalization. To this end, we construct novel physical prior feature maps and explicitly introduce them as an independent modality into the feature space, while maintaining a single-task objective for saliency detection.

Based on the aforementioned challenges and analysis, we propose WaterFlow, a rectified flow-based framework for underwater salient mask generation. WaterFlow can more comprehensively extract spatial semantics from images and endow them with temporal characteristics. By explicitly fusing underwater physical imaging priors with image features, it constructs more comprehensive feature

*Equal Contribution.

† Corresponding author.

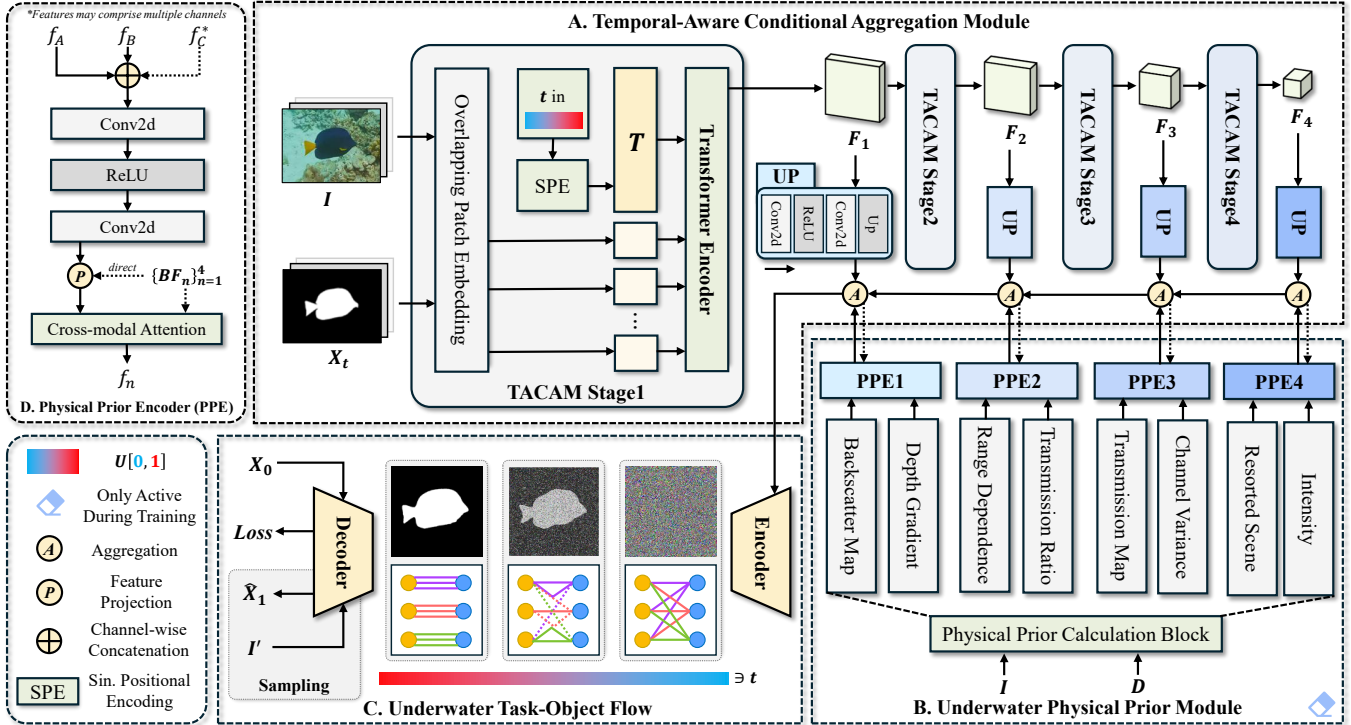


Fig. 2: WaterFlow Architecture. The Temporal-Aware Conditional Aggregation Module (TACAM, defined in Sec. 3.2) and the Underwater Physical Prior Module (UPPM, defined in Sec. 3.3) jointly extract multi-scale features from the input images and masks, which are then fused to guide the downstream Underwater Task Object Flow (UTOF, defined in Sec. 3.4) in generating saliency segmentation masks.

representations, thereby enhancing the performance of SOD tasks. We adopt the Rectified Flow [16] framework to leverage its advantages of linear trajectory learning, achieving more efficient sampling and more stable training processes. Our main contributions are summarized as follows:

- We design a conditional-guided underwater saliency detection model named WaterFlow, which innovatively incorporates underwater physical imaging information as explicit prior knowledge directly into the network training process.
- We are the first to systematically apply Rectified Flow to the challenging field of underwater salient object detection and introduce effective temporal dimension modeling strategies to efficiently meet the diverse feature requirements of different generative stages.
- WaterFlow achieves substantial performance improvements on USOD10K and UFO-120 datasets, reaching state-of-the-art results, which validate its effectiveness and superiority.

2. RELATED WORK

CNN and Transformer-based Segmentation Paradigms. Early methods relied on convolutional neural networks, achieving progress in terrestrial scenarios through multi-scale feature extraction and boundary refinement [12][13][14][17][18]. With the development of self-attention, Transformers were introduced into saliency segmentation and gradually became a new paradigm [19][1]. However, these methods generally ignore underwater imaging physics, and their performance is limited under severe degradations and domain shifts.

Diffusion-based Generative Paradigms. In recent years, diffusion models have shown outstanding performance in image generation, restoration, and segmentation, becoming a major direction in generative modeling [10]. Their step-by-step denoising process produces high-quality results, but low sampling efficiency and unstable training make them unsuitable for real-time and robust underwater detection. Moreover, the incorporation of physical priors remains an open problem.

3. METHOD

3.1. Overall Architecture

We regard SOD as a conditional generation task of saliency masks [11], and accordingly design WaterFlow. As illustrated in Fig. 2, the Temporal-Aware Conditional Aggregation Module (TACAM) progressively extracts multi-scale RGB features through a four-level pyramid structure and fuses them with coarse masks. Meanwhile, the Underwater Physical Prior Module (UPPM), guided by depth information, captures underwater physical priors such as light attenuation, color shift, and scattering, and progressively integrates them with backbone features through a hierarchical strategy. Finally, the downstream Underwater Task Object Flow (UTOF) takes the multi-modal feature maps as conditional input and generates high-quality saliency masks.

3.2. Temporal-Aware Conditional Aggregation Module

TACAM (Fig. 2A) adopts an improved Pyramid Vision Transformer [20] as the backbone network to extract sufficiently discriminative

features, addressing the complex relationship between underwater salient objects and background regions, and obtains the initial spatial embedding $\{OP_n\}_{n=1}^4$. Specifically,

$$OP_n = \begin{cases} Conv2d(R(Conv2d(I) + Conv2d(X_t))), & n = 1 \\ Conv2d(R(Conv2d(OP_{n-1}))), & n = 2, 3, 4 \end{cases} \quad (1)$$

where $R(\cdot)$ denotes the reshape operation.

Traditional diffusion-based methods usually employ fixed features during the reverse process [21]. This static strategy leads to insufficient temporal adaptability of the model: the early steps rely more on global semantic understanding to establish coarse underwater object contours, while the later steps require fine local details to refine boundaries. Inspired by previous work [11], we introduce temporal information as a separate feature embedded into the network:

$$T_n = SPE(t), t \sim U[0, 1] \quad (2)$$

Subsequently, the temporal embedding is concatenated with the spatial embedding and processed through Transformer blocks to obtain $\{F_n\}_{n=1}^4$. F_n passes through UP blocks to finally obtain backbone features $\{BF_n\}_{n=1}^4$. However, underwater scenes present greater complexity than terrestrial environments. To address these domain-specific characteristics, we introduce a dedicated Underwater Physical Prior Module that enhances feature representation by incorporating water-specific knowledge.

3.3. Underwater Physical Prior Module

Light propagation in underwater environments follows complex physical laws [8]. Directly performing saliency segmentation on degraded underwater images often leads to performance degradation when facing complex underwater scenes.

Depth information, as a core element in underwater physical modeling, plays a crucial role in characterizing light propagation and attenuation. Therefore, for the training set I , we employed the state-of-the-art monocular depth estimation model, *Depth Anything V2* [22], to obtain the corresponding depth maps D . The test set remains unprocessed, as this module is only activated during training.

Existing approaches that leverage physical priors mainly follow two strategies: one is to perform complex enhancement preprocessing on raw underwater images and then apply salient object detection on the enhanced images [15][3]; the other is to treat underwater salient object detection and image restoration as parallel tasks and formulate them as a cooperative optimization process [10]. In our view, the former design suffers from information loss and error accumulation, as the separation between enhancement and saliency detection may distort or discard critical details relevant to saliency. Although the latter avoids the drawbacks of serial processing, the inherent inconsistency between the two task objectives often leads to optimization conflicts, preventing physical priors from fully serving the core requirements of saliency detection, while also introducing unnecessary network complexity.

In contrast, we innovatively incorporate physical information as explicit prior knowledge directly into the network, thereby avoiding intermediate information loss and enabling physical constraints to guide saliency determination in a more elegant and precise manner.(Fig. 2B)

Specifically, we model the relationship between underwater captured images and their true versions as:

$$I_c(x) = J_c(x) \cdot T_c^D(x) + A_c \cdot (1 - T_c^B(x)) \quad (3)$$

where $I_c(x)$ represents the pixel intensity of the input image at channel c , and $J_c(x)$ represents its true version. A_c is the background light, whose estimation is based on the dark pixel assumption. $T_c^D(x)$ and $T_c^B(x)$ represent direct transmission and backscattering transmission, respectively [8].

We also extract several common physical features and construct a physical feature set:

$$f = \{B_c(x), \nabla z(x), \beta_c^D, R, T_c^D(x), Var_c, J_c(x), Int\} \quad (4)$$

where $B_c(x)$ represents the backscattering map, $\nabla z(x)$ represents depth gradient, β_c^D represents Range-Dependent Attenuation Coefficient, R represents cross-channel transmission ratio, Var_c represents channel variance, and Int represents backscattering intensity and attenuation intensity maps.

Physical priors injected only at a single scale are difficult to impose effective constraints on both low-level details and high-level semantics simultaneously. Therefore we hierarchically encode physical priors according to semantics:

$$f_n = PPE_n(f_{i|n}), \quad n = 1, 2, 3, 4; \quad i = A, B, C \quad (5)$$

where $f_{i|n} \in f$ represents features i participating in encoding stage n . $PPE_n(\cdot)$ represents the n -th Physical Prior Encoder, whose specific architecture is described in Fig. 2D. Shallow-layer encoding introduces boundary-related physical information such as backscattering and depth gradients, middle layers fuse distance-varying attenuation characteristics and channel difference information, while deep layers impose globally-related physical constraints.

3.4. Underwater Task Object Flow

In the downstream stage, WaterFlow employs an improved conditional generative model based on continuous normalizing flows [16]. Unlike conventional diffusion-based baselines [9], we aim to learn a parameterized conditional vector field network $v_\theta(X_t, t, I)$, which takes as input the position X_t , the time step t , and the condition information I . By solving the ODE $\frac{dX_t}{dt} = v_\theta(X_t, t, I)$, the initial noise distribution π_0 is transformed into the target data distribution $\pi_1(X_t|I)$, i.e., the conditional distribution of the real data X_t given condition I .(Fig. 2C)

Formally, given $X_0 \sim \pi_0$ sampled from the noise distribution and $X_1 \sim \pi_1(X_t|I)$ sampled from the conditional data distribution, we define a straight-line interpolation path:

$$X_t = tX_1 + (1 - t)X_0 \quad (6)$$

where $\forall t \in [0, 1]$. However, Simply using L2 loss pays insufficient attention to boundary accuracy and structural integrity in segmentation tasks [11]. Therefore, we adopt Task Loss as the optimization objective for the network:

$$Loss(\theta) = \frac{1}{2}L_{BCE}(\theta) + \frac{1}{2}L_{IoU}(\theta) \quad (7)$$

Task Loss combines binary cross-entropy and IoU loss, addressing the challenge of underwater object boundary learning by assigning higher weights to boundary regions.

4. EXPERIMENTS

4.1. Experiment Settings

Datasets. We use the USOD10K dataset [1] as the training set to train our model and conduct a comprehensive evaluation on the USOD10K and UFO-120 [23] dataset.

Method	Pub.	USOD10K				UFO-120			
		$MAE \downarrow$	$F^{mean} \uparrow$	$E_{\xi}^{mean} \uparrow$	$S_m \uparrow$	$MAE \downarrow$	$F^{mean} \uparrow$	$E_{\xi}^{mean} \uparrow$	$S_m \uparrow$
MINet [13]	CVPR-20	0.236	0.315	0.573	0.502	0.381	0.299	0.487	0.346
U2-Net [12]	PR-20	0.091	0.650	0.751	0.753	0.219	0.495	0.593	0.598
SUIM-Net [18]	IROS-20	0.130	0.506	0.661	0.637	0.248	0.393	0.521	0.520
SVAM-Net [3]	RSS-22	0.101	0.619	0.735	0.722	0.180	0.640	0.680	0.675
BBRF [14]	TIP-23	0.074	0.776	0.859	0.823	0.203	0.560	0.645	0.641
RMFormer [19]	MM-23	0.083	0.788	0.857	0.829	0.177	0.615	0.676	0.665
TC-USOD [1]	TIP-23	0.086	0.758	0.853	0.816	0.185	0.632	0.712	0.673
MASNet [17]	JOE-24	0.067	0.720	0.801	0.781	0.210	0.543	0.638	0.630
WaterDiffusion [10]	AAAI-25	<u>0.053</u>	0.767	<u>0.875</u>	0.827	0.179	<u>0.654</u>	<u>0.726</u>	<u>0.678</u>
WaterFlow(Ours)		0.026	0.890	0.956	0.899	0.109	0.829	0.832	0.785

Table 1: Quantitative evaluation of various methods across different public underwater datasets, where WaterDiffusion serves as the previous state-of-the-art. The **best** and second-best results are highlighted with bold and underlined, respectively.

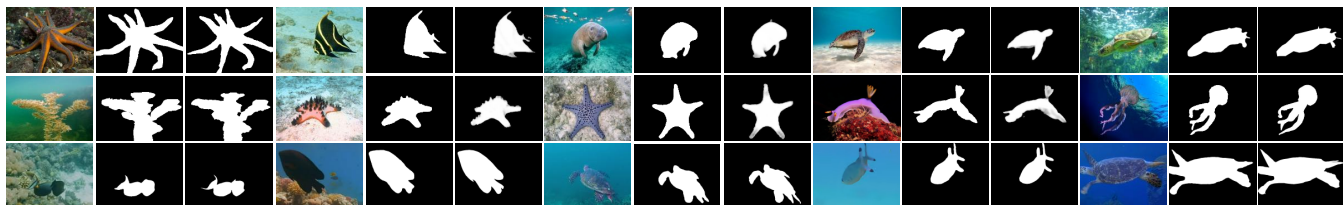


Fig. 3: Qualitative results of saliency detection for our method. In each group of images, the one on the left is the input image, the middle is the segmentation result generated by our model, and the one on the right is the ground truth (GT).

Module		MAE	S_m			
TA	UPPM			Method	Steps	FPS
\times	\checkmark	0.030	0.884	SOTA [10]	1000	2.4
\checkmark	\times	0.034	0.874	Ours	1	20

(a) Component Ablation.

(b) Time Performance.

Table 2: Ablation Study on the USOD10K Dataset.

Evaluation metrics. To comprehensively evaluate the proposed model, we adopt popular metrics for evaluation, including F-measure [24], S-measure [25], E-measure [26], and MAE [27].

Implementation details. We implement our model based on the PyTorch framework, using a single NVIDIA RTX 4090 GPU for training and inference. TACAM is initialized with PVTv2-B4 [20], with input images of 352×352 resolution. We use the AdamW optimizer with a batch size of 8 and gradient accumulation steps of 4. The learning rate is set to 2.5e-5 and training is conducted for 90 epochs. The sampling step is set to 1.

4.2. Evaluation and Ablation Study

Quantitative Evaluation. We compared WaterFlow with nine representative methods on public benchmarks, and the results are shown in Tab. 1. It can be observed that WaterFlow achieves the best performance across all metrics and significantly exceeds the previous state-of-the-art method [10].

Qualitative Evaluation. We provided a comparison with WaterDiffusion in Fig. 1, where its results show foreground misactivation or boundary deviations in certain regions, while WaterFlow produces more accurate and coherent masks. Furthermore, Fig. 3 presents comparisons between WaterFlow and ground truth, demonstrating

that our model can consistently generate high-quality segmentation results across diverse underwater environments.

Ablation and Analysis. Tab.2b compares WaterFlow and WaterDiffusion [10] in terms of sampling steps and FPS performance. WaterFlow achieves over 8× improvement in processing speed while maintaining high accuracy.

We believe that the Temporal-Aware mechanism overcomes the limitations of traditional methods that use a single control image from start to finish by providing adaptive feature inputs at each step during the time-step iteration process of Rectified Flow, enabling the model to dynamically adjust feature representations according to the flow requirements at different time steps. UPPM explicitly integrates the physical prior knowledge of underwater imaging into feature maps, providing the model with richer and more accurate physical constraint information. Furthermore, the adoption of Rectified Flow’s straight-line interpolation strategy significantly improves inference speed. Compared to the complex sampling trajectories of traditional diffusion models, the straight-line path achieves a more efficient generation process [16]. This efficient inference capability is of great significance for the real-time requirements of underwater tasks, enabling it to meet the needs of processing speed-sensitive practical applications such as underwater robot navigation and marine life monitoring.

5. CONCLUSION

We presented WaterFlow, a rectified flow-based model for underwater salient object detection. By explicitly integrating underwater physical priors and temporal modeling, our method achieves more comprehensive feature learning. Experiments on USOD10K and UFO-120 show that WaterFlow outperforms previous SOTA with significant gains. As the first to apply Rectified Flow underwater, we hope that it will be useful for real-time marine work.

6. ACKNOWLEDGMENTS

This work was supported in part by the National Natural Science Foundation of China under Grant 62461018, 62376162; in part by the Hainan Provincial Natural Science Foundation of China under Grant No. 625YXQN594; in part by the Innovation Platform for "New Star of South China Sea" of Hainan Province under Grant No. NHXXRCXM202306; in part by the Research Grants Council of the Hong Kong Special Administrative Region, China under Grant STG5/E-103/24-R.

7. REFERENCES

- [1] Lin Hong, Xin Wang, Gan Zhang, and Ming Zhao, "Usod10k: a new benchmark dataset for underwater salient object detection," *IEEE transactions on image processing*, vol. 34, pp. 1602–1615, 2023.
- [2] Shijie Lian, Hua Li, Runmin Cong, Suqi Li, Wei Zhang, and Sam Kwong, "Watermask: Instance segmentation for underwater imagery," in *ICCV*, Paris, France, Oct. 2023, pp. 1305–1315, IEEE.
- [3] Md Jahidul Islam, Ruobing Wang, and Junaed Sattar, "Svam: Saliency-guided visual attention modeling by autonomous underwater robots," *arXiv preprint arXiv:2011.06252*, 2020.
- [4] Shijie Lian, Ziyi Zhang, Hua Li, Wenjie Li, Laurence Tianruo Yang, Sam Kwong, and Runmin Cong, "Diving into underwater: Segment anything model guided underwater salient instance segmentation and a large-scale dataset," in *ICML*, 2024, pp. 29545–29559.
- [5] Avishek Siris, Jianbo Jiao, Gary KL Tam, Xianghua Xie, and Rynson WH Lau, "Scene context-aware salient object detection," in *ICCV*, 2021, pp. 4156–4166.
- [6] Yi Wang, Ruili Wang, Xin Fan, Tianzhu Wang, and Xiangjian He, "Pixels, regions, and objects: Multiple enhancement for salient object detection," in *CVPR*, June 2023, pp. 10031–10040.
- [7] Ziyang Luo, Nian Liu, Wangbo Zhao, Xuguang Yang, Dingwen Zhang, Deng-Ping Fan, Fahad Khan, and Junwei Han, "Vscore: General visual salient and camouflaged object detection with 2d prompt learning," in *CVPR*, June 2024, pp. 17169–17180.
- [8] Derya Akkaynak and Tali Treibitz, "Sea-thru: A method for removing water from underwater images," in *CVPR*, June 2019.
- [9] Jonathan Ho, Ajay Jain, and Pieter Abbeel, "Denoising diffusion probabilistic models," *Advances in neural information processing systems*, vol. 33, pp. 6840–6851, 2020.
- [10] Laibin Chang, Yunke Wang, Longxiang Deng, Bo Du, and Chang Xu, "Waterdiffusion: Learning a prior-involved unrolling diffusion for joint underwater saliency detection and visual restoration," in *Proceedings of the AAAI Conference on Artificial Intelligence*, 2025, vol. 39, pp. 1998–2006.
- [11] Zhongxi Chen, Ke Sun, and Xianming Lin, "Camodiffusion: Camouflaged object detection via conditional diffusion models," in *Proceedings of the AAAI Conference on Artificial Intelligence*, 2024, vol. 38, pp. 1272–1280.
- [12] Xuebin Qin, Zichen Zhang, Chenyang Huang, Masood Dehghan, Osmar R Zaiane, and Martin Jagersand, "U2-net: Going deeper with nested u-structure for salient object detection," *Pattern recognition*, vol. 106, pp. 107404, 2020.
- [13] Youwei Pang, Xiaoqi Zhao, Lihe Zhang, and Huchuan Lu, "Multi-scale interactive network for salient object detection," in *CVPR*, 2020, pp. 9413–9422.
- [14] Mingcan Ma, Changqun Xia, Chenxi Xie, Xiaowu Chen, and Jia Li, "Boosting broader receptive fields for salient object detection," *IEEE Transactions on Image Processing*, vol. 32, pp. 1026–1038, 2023.
- [15] Jinkang Wang, Xiaohui He, Faming Shao, Guanlin Lu, Ruizhe Hu, and Qunyan Jiang, "Semantic segmentation method of underwater images based on encoder-decoder architecture," *Plos one*, vol. 17, no. 8, pp. e0272666, 2022.
- [16] Xingchao Liu, Chengyue Gong, and Qiang Liu, "Flow straight and fast: Learning to generate and transfer data with rectified flow," *arXiv preprint arXiv:2209.03003*, 2022.
- [17] Zhenqi Fu, Ruizhe Chen, Yue Huang, En Cheng, Xinghao Ding, and Kai-Kuang Ma, "Masnet: A robust deep marine animal segmentation network," *JOE*, vol. 49, no. 3, pp. 1104–1115, 2023.
- [18] Md Jahidul Islam, Chelsey Edge, Yuyang Xiao, Peigen Luo, Muntaqim Mehtaz, Christopher Morse, Sadman Sakib Enan, and Junaed Sattar, "Semantic segmentation of underwater imagery: Dataset and benchmark," in *IROS*. IEEE, 2020, pp. 1769–1776.
- [19] Xinhao Deng, Pingping Zhang, Wei Liu, and Huchuan Lu, "Recurrent multi-scale transformer for high-resolution salient object detection," in *ACM MM*, 2023, pp. 7413–7423.
- [20] Wenhai Wang, Enze Xie, Xiang Li, Deng-Ping Fan, Kaitao Song, Ding Liang, Tong Lu, Ping Luo, and Ling Shao, "Pvt v2: Improved baselines with pyramid vision transformer," *Computational visual media*, vol. 8, no. 3, pp. 415–424, 2022.
- [21] Tomer Amit, Tal Shaharbany, Eliya Nachmani, and Lior Wolf, "Segdiff: Image segmentation with diffusion probabilistic models," *arXiv preprint arXiv:2112.00390*, 2021.
- [22] Lihe Yang, Bingyi Kang, Zilong Huang, Zhen Zhao, Xiaogang Xu, Jiashi Feng, and Hengshuang Zhao, "Depth anything v2," in *Advances in Neural Information Processing Systems*, A. Globerson, L. Mackey, D. Belgrave, A. Fan, U. Paquet, J. Tomczak, and C. Zhang, Eds. 2024, vol. 37, pp. 21875–21911, Curran Associates, Inc.
- [23] Md Jahidul Islam, Peigen Luo, and Junaed Sattar, "Simultaneous enhancement and super-resolution of underwater imagery for improved visual perception," *arXiv preprint arXiv:2002.01155*, 2020.
- [24] Radhakrishna Achanta, Sheila Hemami, Francisco Estrada, and Sabine Susstrunk, "Frequency-tuned salient region detection," in *CVPR*. IEEE, 2009, pp. 1597–1604.
- [25] Deng-Ping Fan, Ming-Ming Cheng, Yun Liu, Tao Li, and Ali Borji, "Structure-measure: A new way to evaluate foreground maps," in *ICCV*, 2017, pp. 4548–4557.
- [26] Deng-Ping Fan, Cheng Gong, Yang Cao, Bo Ren, Ming-Ming Cheng, and Ali Borji, "Enhanced-alignment measure for binary foreground map evaluation," *arXiv preprint arXiv:1805.10421*, 2018.
- [27] Federico Perazzi, Philipp Krähenbühl, Yael Pritch, and Alexander Hornung, "Saliency filters: Contrast based filtering for salient region detection," in *CVPR*. IEEE, 2012, pp. 733–740.